*Tellus* (1981), *33*, 1–11

# Some basic experiments with a vertically-integrated ice sheet model

By J. OERLEMANS,† *Royal Netherlands Meteorological Institute, Postbus 201, De Bilt, The Netherlands*

(Manuscript received March 11; in final form June 4, 1980)

ABSTRACT

A simple 1½-dimensional continental ice sheet model is presented. The model is based on Nye's (1959) proposal to express the vertical mean horizontal ice-velocity as $u = B\tau_b^m$, where $\tau_b$ is the basal shear stress and $B$ and $m$ are constants. Essentially, the spread of ice is governed by a nonlinear diffusion equation for the ice thickness. The diffusivity increases with both ice thickness and surface slope. In one direction ($y$) a typical scale is prescribed that governs the lateral ice-mass discharge, whereas in the other direction ($x$) the ice-sheet evolution is computed explicitly on a grid with a spacing of 70 km.

A series of experiments has been carried out with various boundary conditions and parameterizations of the annual mass balance. It appears that the boundedness of continents and bedrock elevations creates a strongly nonlinear response of ice sheets to climatic variations. The behaviour of Northern Hemisphere ice sheets as computed with the numerical model is compared to that predicted by a perfect-plasticity model. It is found that those models give qualitatively the same results.

Including bedrock sinking in a simple way reveals that this causes Northern Hemisphere ice sheets to disappear spontaneously within 15,000 years, after about 50,000 years of growth (initiated by a cold period).

## 1. Introduction

A growing interest exists in the behaviour of large continental ice sheets. They play an important role in the climate system through their interaction with the atmosphere. Although ice sheet and glacier modelling has reached some degree of sophistication, existing models have been used primarily in studies of the present day ice sheets of Greenland and Antarctica, and of glacier surges (see Budd and Radok (1971) for a review). With regard to climate studies, use has been made of perfectly plastic ice sheets, e.g. Weertman (1961, 1976), Birchfield (1977) and Pollard (1978). In those studies, the dependence of the mass balance on height is incorporated and appears to provide a strong positive feedback in ice-sheet growth. Recently, Andrews and Mahaffy (1976) and Oerlemans (1980a) have studied the possibility of rapid growth of the Laurentide and Scandinavian ice sheets, respectively. They used simple vertically integrated models.

In this study some basic experiments carried out with a simplified version of the model described in Oerlemans (1980a) will be discussed. This simplification serves to reduce computational times and is suitable for the type of experiments to be discussed here. The emphasis will be on ice-sheet behaviour under various boundary conditions. It is not the intention to study the mechanics of ice flow, but to investigate the large scale behaviour of ice sheets that is immediately relevant from the viewpoint of dynamical climatology.

## 2. Description of the model

The ice-sheet model to be used will be described briefly. For further background on ice-flow mechanics and the problems involved, the reader is referred to Paterson (1969) and Budd and Radok (1971).

† Currently at: IMOU, State University of Utrecht. Princetonplein 5, Utrecht, The Netherlands.

 0040-2826/81/010001-11$02.50/0 

The model is based on Nye's (1959) proposal to combine the effects of internal deformation within the ice and sliding at the bottom by using a simple flow law of the type

$$u = B\tau_b^m. \tag{1}$$

In (1), $u$ is the vertical mean (= from the bottom to the top of the ice sheet) velocity and $\tau_b$ is the shear stress at the bottom. In principle, the constant $B$ depends on the temperature distribution in the ice. The value of $m$ is more constant, although it depends slightly on the relative contribution of basal sliding to the vertical mean velocity. Current values of $m$ are between 2 and 3.

In the present model the temperature distribution in the ice is not computed, so the only possibility of using (1) is to keep $B$ and $m$ at constant values. This implies for example that ice-sheet surges cannot occur in the model. Throughout this study it is also assumed that ice density is constant, which means that mass flow and volume flow are equivalent concepts.

For large ice sheets longitudinal stresses are generally small, which suggests to generalize (1) for the two-dimensional case. Since the basal shear stress is proportional to $H\nabla H^*$, where $H$ is the ice thickness and $H^*$ the elevation of the ice surface above sea level, the vertically integrated mass-flow vector $\mathbf{M}$ becomes

$$\mathbf{M} = A H^{m+1} |\nabla H^* \cdot \nabla H^*|^{(m-1)/2} \nabla H^*. \tag{2}$$

The constant $A$ is just an optimum value of $B$ for the two-dimensional case. Due to the nonlinear character of ice flow, these constants need not be equal.

The evolution of the ice sheet is described by the conservation of ice mass, which reads

$$\frac{\partial H}{\partial t} = \nabla \cdot \mathbf{M} + G. \tag{3}$$

Here, $G$ denotes the (annual mean) mass balance. Equations (2) and (3), together with the condition that $H \geqslant 0$, completely describe the model.

A more transparent formulation of the model is obtained by the consideration that the transport of ice mass, from accumulation to ablation regions, is essentially a diffusive process, with a positive but variable diffusivity. Writing

$$\frac{\partial H}{\partial t} = \nabla \cdot D\nabla H^* + G \tag{4}$$

the diffusivity $D$ is found to be

$$D = A H^{m+1} \left[ \left( \frac{\partial H^*}{\partial x} \right)^2 + \left( \frac{\partial H^*}{\partial y} \right)^2 \right]^{(m-1)/2} \tag{5}$$

So the spread of ice is described by a nonlinear diffusion equation, and the diffusivity increases with the slope of the ice surface and in particular with the ice thickness. The latter implies that $D$ tends to be larger in the higher parts of the sheet, which causes the ice-sheet edge to be steep compared to what a linear (= constant $D$) diffusion equation would give. In general, ice sheets show a tendency to reduce variations in $D$ by having larger surface slopes if the thickness is smaller. At this point it is interesting to recall that for a perfectly plastic ice sheet the product $H\partial H/\partial x$ is constant (e.g. Paterson, 1969).

The model described above is two-dimensional and has been used in a study of the Scandinavian ice sheet (Oerlemans, 1980a). In order to reduce computational times, this model is now simplified.

The coordinate axes are chosen in such a way that the ice sheet evolution is most pronounced along the $x$-axis. For the American and Eurasian continental ice sheets, this will be the north-south direction. In the lateral direction, i.e. along the $y$-axis, the spatial scale of the ice sheet is prescribed, it is denoted by $Y$ (see Fig. 1). If the $x$-axis is placed over the highest part of the sheet, and if variations of the bedrock height are not too pronounced in the $y$-direction, the approximations $\partial H^*/\partial y \simeq 0$ and $\partial^2 H^*/\partial y^2 \simeq H/Y^2$ may be used. Inserting this in (4) and (5) yields for the simplified model:

$$\frac{\partial H}{\partial t} = \frac{\partial}{\partial x} D' \frac{\partial H^*}{\partial x} + D' H/Y^2 + G, \tag{6}$$

where

$$D' = A H^{m+1} \left( \frac{\partial H^*}{\partial x} \right)^{m-1}. \tag{7}$$

Equations (6) and (7) formulate a $1\frac{1}{2}$-dimensional model. Lateral discharge of ice mass is still possible through the $D' H/Y^2$-term in (6). In principle $Y$ may be a function of $x$, or even of $t$. For example, in some cases it may be realistic to let $Y$ grow with $H$. If $Y \to \infty$ the model becomes one-dimensional. In some experiments this version will be used.

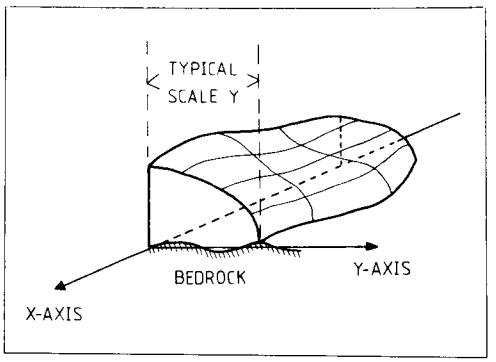


*Fig. 1.* Sketch of an ice sheet and its orientation in the coordinate system. The scale $Y$ determines the lateral ice-mass discharge.

The flow law (1) is only valid if the ice thickness is at least a few hundred meters and longitudinal stresses are small. This implicates that (1) does not hold at the edge and at the centre of an ice sheet. Moreover, (6) does not allow the ice sheet to grow if $G \leqslant 0$ at the edge, because here $D = 0$. To avoid such unrealistic behaviour, the condition $D' \geqslant D'_0$ is added to (7). In all experiments, $D'_0$ was set equal to the diffusivity corresponding to a surface slope of $2*10^{-3}$ and an ice thickness of 500 m. Some sensitivity experiments showed that the evolution of a model ice sheet does not depend strongly on the choice of $D'_0$.

Equations (6) and (7) are solved on a grid with a spacing of 70 km. An explicit forward scheme is used for the time integration, and spatial derivatives are approximated by central differencing. With a time step of 20 years, and without any smoothing, the scheme appeared to be stable for all experiments of interest. For some further discussion on the numerical method, see Oerlemans (1980a).

## 3. Some basic experiments

In interpreting the results, it should be realized that $A$ and $m$ govern two characteristic quantities of the model ice sheet, namely, its height-to-width ratio and the steepness of the edge. Therefore, $A$ and $m$ were chosen in such a way that the model gives realistic values of those quantities. It turned out that taking $m = 2.5$ and $A = 1$ m$^{-3/2}$ yr$^{-1}$ did meet this requirement.

As a first experiment, an ice sheet was computed for a flat continent bounded by deep ocean ($H(t) \equiv 0$). The size of the continent was taken to be 2030 km. The net mass balance was set to 0.3 m/yr, and the initial condition was $H(x) = 0$. The pure one-dimensional model version was used ($Y = \infty$). The configuration sketched above resembles the situation in the Antarctic region.

Fig. 2 shows the steady-state solution, reached after approximately 20,000 years. Since the sheet is symmetric with respect to its centre only one-half is shown. For comparison, the dashed line shows an ice-sheet profile obtained from a linear diffusion equation with a diffusivity chosen such that $H_{max}$ is equal to that for the nonlinear case. Apparently, the linear model does not produce a steep edge. Other experiments not shown here brought to light that differences between linear and nonlinear models may be very large for developing or decaying sheets; this is physically quite clear.

Also shown is the diffusivity $D'$. It reaches a maximum value halfway between the ice sheet's centre and edge. At the centre and edge $D' \to 0$ because $\partial H/\partial x \to 0$ and $H \to 0$, respectively. In the model, $D'$ is set to $D'_0$ at these locations, but

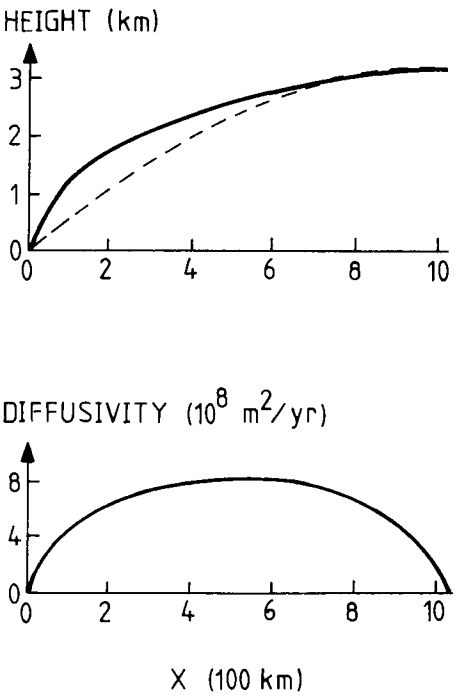


*Fig. 2.* Upper panel: ice-sheet profile of a steady-state ice sheet computed with the nonlinear model (solid line) and a linear model (dashed line). Lower panel: diffusivity for the nonlinear case.

since $D_0' = 0.25*10^6$ m$^2$/yr it appears as zero in the figure.

The experiment was repeated for other values of the mass balance $G$. Fig. 3 shows how in the steady state the surface height at the centre of the sheet ($H_{max}$) depends on $G$. The dependence is rather weak, suggesting that the height of the Antarctic ice sheet is rather insensitive to variations in $G$. This is a well-accepted point (e.g. Flint, 1971). It should be noted that a perfectly plastic ice sheet would not react to variations in $G$ at all—its shape is fully determined by its size.

Although the equilibrium ice-sheet height hardly depends on $G$, this does not apply to the time needed to reach equilibrium. It ranges from 45,000 years for $G = 0.1$ m/yr to 10,000 years for $G = 1$ m/yr.

In the second experiment, the continent was bounded by deep ocean at one side only, namely at $x = 0$. This configuration may be seen as representative for Northern Hemisphere conditions, with $x = 0$ at the coast of the Arctic Sea and the $x$-axis pointing southward. The lateral scale $Y$ was taken to be 1000 km. The mass balance was prescribed as

$$G = 0.4 - 0.3*10^{-6}\, x \ \ m/yr, \tag{8}$$

so it decreases linearly from 0.4 m/yr at $x = 0$ to −0.3 m/yr at $x = 2500$ km. The equilibrium point, defined here as the location on the $x$-axis where $G = 0$, was thus located at $x = 1333$ km. Equation (8) is not meant to represent real conditions, but is employed merely to carry out a simple "academic" experiment. More realistic representations of $G$ in which height dependence is included will be used later.

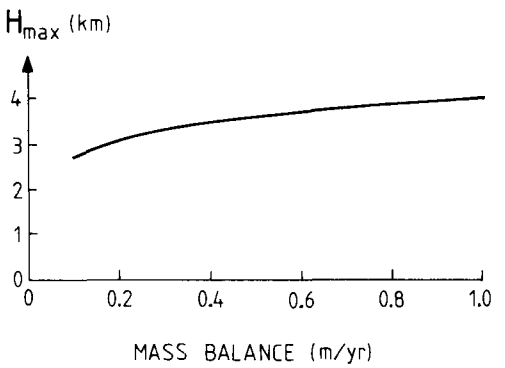


*Fig. 3.* Surface elevation (= ice thickness) at the centre of the sheet, as a function of the annual mass balance.

Steady-state profiles for this experiment are shown in Fig. 4. The upper profile is for a perfectly flat base, the lower one for the case of a bedrock elevation as indicated. Due to the $x$-dependency of $G$, the sheet is not symmetric: the edge of the ablation side is less steep. The presence of the mountain range allows the ice to penetrate further south. In this case, the enhanced shear stress on the mountain slope creates a local minimum in $H$ at $x = 900$ km, while the sheet reaches its maximum thickness at $x = 1200$ km.

In order to get an idea of how the computed steady-state depends on the model parameters, some runs were carried out with other values of $A$ and $Y$, while the boundary conditions were kept the same (only the case with a flat base was run). Table 1 lists some results. Increasing the value of $A$ leads to a lower ice sheet, while its size is hardly affected (not within the model resolution of 70 km). For a small lateral scale $Y$, both $H_{max}$ and $L$ are small. Larger $Y$ implicates less ice-mass discharge in the lateral direction, so $H_{max}$ and $L$ increase. The one-dimensional case ($Y \to \infty$) does not differ very much from the case with $Y = 1000$ km, i.e. an ice-sheet width of 2000 km.

## 4. Height-dependent mass balance

The behaviour of ice sheets becomes far more interesting if the dependence of the mass balance on surface height is taken into account. This adds

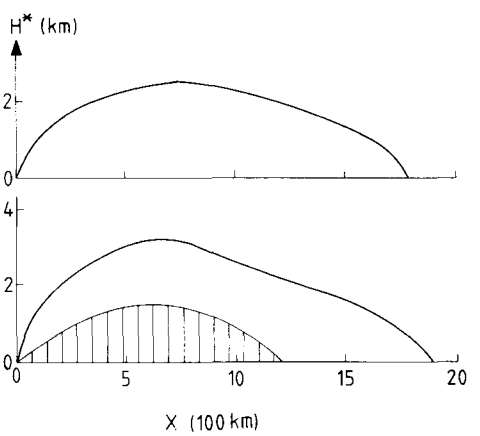


*Fig. 4.* Steady-state ice-sheet profiles for a mass balance depending on $x$ only. The equilibrium point is located at $x = 1333$ km. The upper panel shows the case with a flat bedrock, the lower one the case with a mountain range (all other things being equal).

Table 1. *Maximum height* ($H_{max}$ *in m) and size* (L *in km) for various values of the model parameters* A *and* Y (*units* $m^{-3/2}$ $yr^{-1}$ *and km, respectively*). *See text for further description of the experiment*

| | | $H_{max}$ (m) | L (km) |
|---|---|---|---|
| $Y = 1000$ | $A = 0.2$ | 3240 | 1750 |
| | $A = 1$ | 2489 | 1750 |
| | $A = 2$ | 2217 | 1750 |
| | $A = 3.5$ | 2020 | 1750 |
| $A = 1$ | $Y = 100$ | 1402 | 1400 |
| | $Y = 500$ | 2207 | 1610 |
| | $Y = 1000$ | 2489 | 1750 |
| | $Y \to \infty$ | 2690 | 1890 |

an essentially nonlinear element, which is now included into a study of the Northern Hemisphere ice sheets.

The height dependence of the mass balance is prescribed as

$$G = 0.73*10^{-3}*(h - E) + 0.27*10^{-6}*(h - E)^2 \quad \text{m/yr} \tag{9}$$

where $h$ and $E$ are in meters. $E$ is the height of the equilibrium line (defined by $G = 0$); it depends on $x$, see Fig. 5. The maximum value of $G$ is 0.5 m/yr for $h - E = 1500$ m; for larger values of $h - E$, $G$ is kept at this value.

A few considerations led to employing a parabolic height dependence of $G$ as formulated by (9). Observations have shown that an upper limit to precipitation amounts exists if one goes upward. The reason for this simply is the decreasing water vapour content of the air. For the same reason precipitation amounts in the polar regions are small. Characteristic values of the present yearly precipitation are 0.3 m/yr in the Antarctic and 0.5 m/yr in the Arctic.

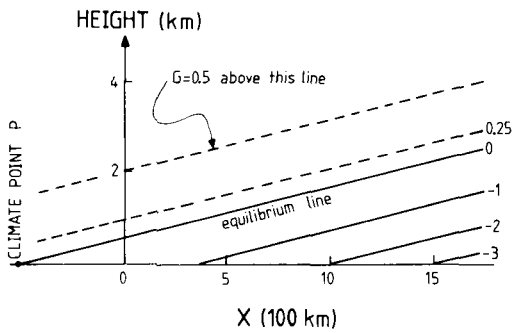


*Fig. 5.* Parameterization of the mass balance $G$. Unit is m/yr. The point where the equilibrium line intersects the sea level is called the "climate point" and is denoted by $P$.

Mass balance studies of mountain glaciers yield widely varying results depending on the exposure of the glacier to local effects. The general picture is that $G$ increases less rapidly than linear with height. However, it is very questionable whether measurements on today's valley glaciers are representative for the conditions that surrounded the large Northern Hemisphere ice sheets.

Experiments with an ice/snow melt model carried out by the author (Oerlemans and Bienfait, 1980) have shown that the dependence of ice melt on surface elevation can be fitted with a parabolic curve quite well. It also appeared that this height dependence is conserved if the Milankovitch insolation variations are imposed. Altogether, the parabolic profile of $G$ seems to be most satisfying at present, but the coefficients remain subject to ambiguity.

The height of the equilibrium line is expressed as a linear function of $x$ (the $x$-axis pointing southward again) according to

$$E(x) = \theta(x - P). \tag{10}$$

The value of $\theta$ is positive, so $E$ decreases with latitude. $P$ indicates where the equilibrium line intersects sea level. It is called the "climate point" because in a later stage it will serve as an indicator for the prevailing climatic conditions. The slope of the equilibrium line ($\theta$) is in the $0.5*10^{-3}$ to $10^{-3}$ range. Data presented by Charlesworth (1957) suggest a value of $0.5*10^{-3}$, whereas Weertman (1976) uses a value of $10^{-3}$; the experiments with the ice/snow melt model mentioned above suggest a value close to the first one.

The parameterization of the mass balance given by eqs. (9) and (10) is of course schematic. It should be emphasized that it is no fit to some field experiment but meant to reflect the overall picture. It should be sufficiently accurate to investigate the principal effect of the height-mass balance feedback. At this point it should be noted that a similar type of mass-balance representation was used by Andrews and Mahaffy (1976) in a study of the growth of the Laurentide Ice Sheet.

Fig. 5 shows an example of the distribution of $G$.

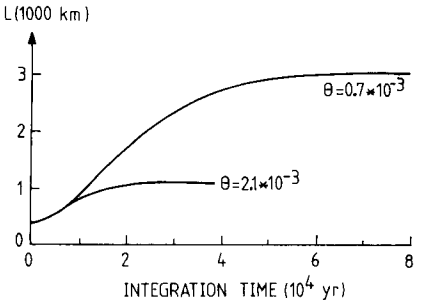


*Fig. 6.* Evolution of the model ice sheet for two values of the slope of the equilibrium line $\theta$. Initial conditions: $H(x) = 0$.

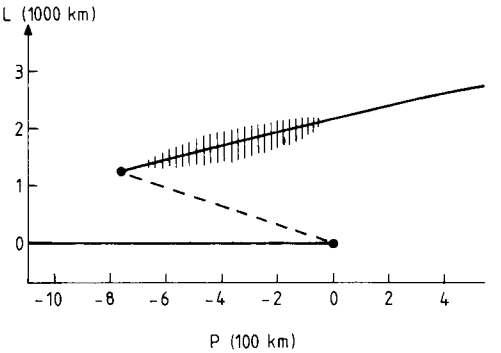


*Fig. 7.* Solution diagram with respect to $P$ for Northern Hemisphere ice sheets. Solid lines and dashed line indicate stable and unstable equilibrium solutions, respectively. In the shaded region the ice sheet behaves almost intransitively.

The transition from polar sea to continent, which is somewhere between 70 and 75° N, is located at $x = 0$. The example shown reflects conditions very close to present: the climate point is located well in the polar sea.

With this parameterization of the mass balance, runs were carried out with various values for $\theta$ and $P$. With a flat bedrock and initial condition $H(x) = 0$, an ice sheet develops only if $P > 0$, i.e. if the climate point is located on the continent. The steady-state size and the time necessary to reach it are very sensitive to $\theta$, the slope of the equilibrium line. Fig. 6 illustrates this point. It shows the ice-sheet growth for $\theta = 0.7*10^{-3}$ and $\theta = 2.1*10^{-3}$, with $P = 350$ km and $Y = 1000$ km in both cases. Obviously, a smaller slope increases both the time scale and the equilibrium ice-sheet size. Since a smaller slope of the equilibrium line implicates a stronger feedback between southward ice-sheet growth and mass balance, this result is not unexpected. In the extreme case of an equilibrium line running parallel to the surface ($\theta = 0$), the ice sheet will grow to infinity once it has reached a certain critical mean height.

The height–mass balance feedback creates a strong nonlinearity in the model. It may therefore be possible that, for given values of $P$ and $\theta$, more than one equilibrium solution exists. This point has already been noted by Bodvarsson (1955) and Weertman (1961). In order to see whether the present model possesses regions with multiple solutions, many runs were carried out with different initial conditions. The emerging solution diagram (with respect to $P$) is shown in Fig. 7. The slope of the equilibrium line was fixed at $0.84*10^{-3}$. The value of $P$ (horizontal axis) may be thought to reflect the climatic conditions. Apparently, the ice sheet shows hysteresis. For very warm conditions ($P < -750$ km) no ice sheet is possible ($L = 0$). For moderate conditions ($-750 < P < 0$ km), three solutions exist: $L = 0$, $L =$ small and $L =$ large; the solution with a small ice sheet is unstable (dashed line). Finally, for cold ($P > 0$ km) conditions only a large sheet is possible. A similar behaviour was found by Weertman (1976) for a perfectly plastic ice sheet with a step function of $G$, i.e. regions of constant accumulation and ablation separated by the equilibrium line.

The shaded region in Fig. 7 indicates a region where the model ice-sheet behaves almost intransitive. That is, within this region the convergence to the equilibrium solution is extremely slow. This is due to the fact that the average mass balance remains practically zero if the sheet is made somewhat larger or smaller.

Some observational evidence exists that the cryosphere has two states of preference. From a Carribean deep-sea core, Imbrie et al. (1974) found that the frequency distribution of sea-surface temperature (over the last 450,000 yrs) shows a uni-modal shape while that of global ice-volume shows a bi-modal shape. This is in accordance with Fig. 7. If climatic variations are such that $P$ runs back and forth along the $x$-axis, a bi-modal distribution of the ice volume should be expected (changes in global ice volume are due mainly to changes in the American and Eurasian ice sheets (e.g. Flint, 1971). The observational data thus seem to support the model results displayed in Fig. 7.

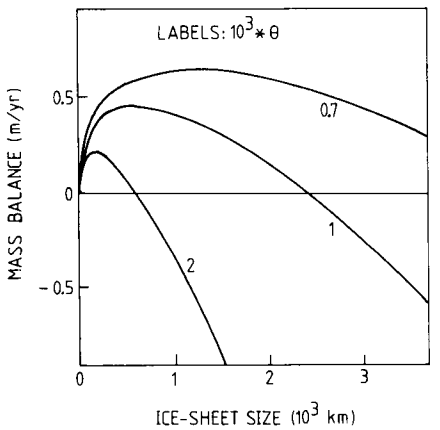


*Fig. 8.* Mass balance of the southern half of a perfectly plastic ice sheet, for three values of the slope of the equilibrium line.

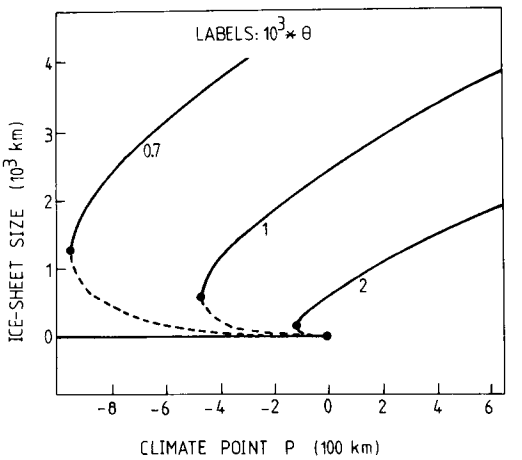


*Fig. 9.* Solution diagram for Northern Hemisphere ice sheets according to perfect-plasticity theory (compare Fig. 7).

In order to get a better understanding of how the hysteresis is established, and to see how its shape depends on some model parameters, an analytical derivation will be discussed in the next section.

## 5. Comparison to perfect-plasticity theory

The shape of a perfectly plastic ice sheet is fully determined by its size $L$ according to (e.g. Weertman, 1976)

$$H(x) = \sigma\{\tfrac{1}{2}L - |x - \tfrac{1}{2}L|\}^{1/2}. \tag{11}$$

The constant $\sigma$ depends on the yield stress of ice and determines the height to width ratio, in analogy to the constant $A$ in the numerical model. Equation (11) follows directly from the requirement that the shear stress at the bottom equals the yield stress everywhere. In the equilibrium case the flux of ice mass through the centre of the sheet is zero, implying that the ice-sheet size can be found by making up the mass balance over the southern half.

The mass balance is now taken linear with respect to height, so

$$G = \alpha(x - P) + \beta h \tag{12}$$

The slope of the equilibrium line is given by $\theta = -\alpha/\beta$. Since $H(x)$ is uniquely related to $L$, the average mass balance over the southern half, denoted by $G^*$, can also be uniquely related to $L$. Equilibrium solutions are then found by the requirement $G^* = 0$; they are stable if $\partial G^*/\partial L < 0$ and unstable if $\partial G^*/\partial L > 0$.

Substitution of $H(x)$ from (11) for $h$ in (12) and integration from $x = \frac{1}{2}L$ to $x = L$ yields

$$G^*(L) = B_1 + B_2 L^{1/2} + B_3 L, \tag{13}$$

where

$$B = -\alpha P$$
$$B_2 = 0.47\,\beta\sigma$$
$$B_3 = 0.75\,\alpha$$

Equation (13) shows that variations in $P$ shift the $G^*(L)$-curve up and down without affecting its shape. Therefore the case $P = 0$ is considered first. Fig. 8 shows how $G^*$ depends on $L$ for various values of $\theta(\beta = 10^{-3}\ \mathrm{y}^{-1}$ and $\sigma = 2.5\ \mathrm{m}^{1/2})$. The equilibrium solutions are given by the intersections of the $G^*(L)$-curve with $G^* = 0$. As was found earlier with the numerical model, the ice-sheet size increases strongly if the slope of the equilibrium line ($\theta$) decreases.

Since $\alpha < 0$, a positive value of $P$ implies that the $G^*(L)$-curve shifts upward and that the equilibrium ice-sheet size increases. On the other hand, if $P < 0$ two equilibrium solutions appear: a small and a large sheet. The small sheet is unstable because $\partial G^*/\partial L > 0$ for this state. For large negative values of $P$, i.e. if the climate point is located far in the polar sea, the $G^*(L)$-curve lies completely below $G^* = 0$. In this case no ice sheet is possible.

With the observation that $L = 0$ is always a stable solution if $P < 0$, a solution diagram can now be constructed. The equilibrium solutions are easily found by setting $G^* = 0$ in (13) and squaring. Fig. 9 shows the result for three values of $\theta$. The solution diagram is essentially the same as that shown in Fig. 7 (where $\theta = 0.84*10^{-3}$ was used), although the equilibrium size depends much stronger on $P$. This is due to both differences in the shape of the ice sheet and differences in the formulation of $G$. Altogether, however, the characteristics of the numerical and analytical models are rather similar.

The position of the critical point $P_{crit}$, below which no ice sheet is possible, is found by equating the determinant of (13) to zero. This yields

$$P_{crit} = -0.74\, \sigma^2 \beta^2/\alpha^2. \qquad (14)$$

So for $P < P_{crit}$, the only solution is $L = 0$. Note that $P_{crit}$ is always negative. Equation (14) shows directly that the hysteresis becomes more pronounced if the slope of the equilibrium line ($\theta = -\alpha/\beta$) is smaller.

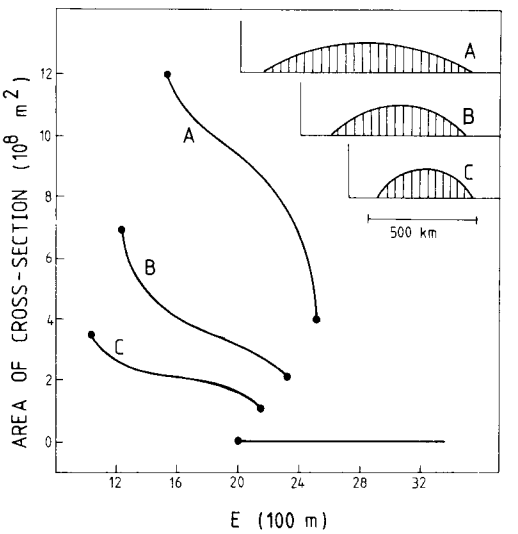


*Fig. 10.* Solution diagram for ice sheets over various kinds of mountain ranges. In each case the mountain height is 2000 m, but horizontal scales are different as indicated.

## 6. The effects of mountains

The analysis of the foregoing sections shows that the response of continental ice sheets to climatic variations may be strongly nonlinear. An important question now is how the presence of mountain ranges can modify the picture.

The hysteresis displayed in Figs. 7 and 9 would not appear if (i) $G$ would not depend on surface elevation, and (ii) if the continent was not bounded by the polar sea. It may be expected that other boundary conditions, like mountain ranges, can exert a pronounced influence on the solution diagram.

In order to isolate the effect of mountains, some numerical experiments were carried out with $\theta = 0$, i.e. with the lines of equal mass balance parallel to the geoid. Consequently, only the height of the equilibrium line ($E$) is the relevant climatic parameter. Mountain ranges were introduced by prescribing a surface elevation of parabolic shape as shown in the upper right of Fig. 10. The land on both sides of the mountain extended to infinity, while the lateral scale $Y$ was taken to be 1000 km.

Before discussing the solution diagram, a few considerations may be useful. First, one should realize that if no mountains were present, the case $\theta = 0$ can never give a steady-state ice sheet—there will be no ice sheet at all or it will grow to infinity. If mountains are introduced, however, stable ice sheets are possible because the surface height–mass balance feedback can be cancelled by larger ice-mass discharge due to the mountain slopes. So if initially no ice sheet exists and then the equilibrium line comes down ($E$ decreases) and reaches the mountain top, a small cap may form and reach a steady state. If $E$ is dropped further, a critical point will be reached where the ice sheet starts to grow to infinity. If the equilibrium line is raised again, a small ice cap may remain even if $E$ is slightly higher than the mountain top—in this case the thickness of the cap keeps a part of its surface in the accumulation zone.

Fig. 10 shows the solution diagram, with respect to $E$, for three types of mountains. In each case the mountain height is 2000 m, but the horizontal scales are different. The ice-sheet size is expressed in terms of the cross-section area in the $x$-direction.

For a small mountain a stable ice cap may exist if $1050 < E < 2150$ m. If $E > 2150$ no cap is possible and if $E < 1050$ m it grows to infinity. For larger mountains, i.e. for smaller slopes. the critical points shift towards higher values of $E$. Of course the precise position of the critical points

depends on the ice-flow parameters $A$ and $m$, but some sample calculations showed that this dependence is rather weak. The general conclusion should therefore be that mountain ranges introduce another nonlinearity in the cryosphere. This makes the total picture rather complicated. As an illustration, consider the case of Scandinavia.

At present, part of Scandinavia consists of high mountain regions up to 2000 m. In accordance with the preceding section, this should give rise to hysteresis (Fig. 10). On the other hand, since the Scandinavian continent is bounded by the polar sea, the type of hysteresis discussed in Sections 4 and 5 will also occur. As a consequence, for a certain range of climatic conditions the Scandinavian sheet will have three stable equilibrium solutions. Fig. 11 illustrates this rather complicated behaviour. Experiments with a two-dimensional model of the Scandinavian ice sheet (Oerlemans, 1980a) indicate that this type of behaviour indeed occurs.

## 7. Isostatic adjustment of the bedrock

So far it has been assumed that the bedrock does not react to the load of ice mass. In reality there is of course the tendency to restore isostatic equilibrium. In the simplest form this may be formulated by

$$\frac{\partial h}{\partial t} = -\omega(H^* + 2h) \tag{15}$$

where $h$ is the height of the bedrock with respect to its equilibrium value (the case of no ice sheet).

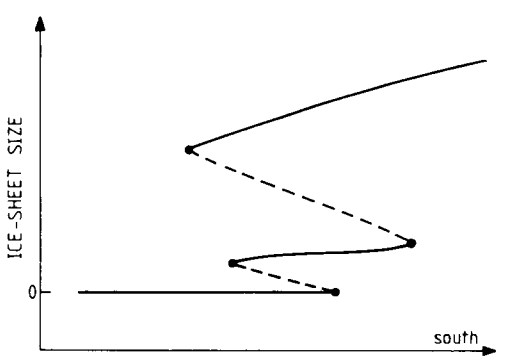


*Fig. 11.* Schematic solution diagram for the Scandinavian ice sheet, combining the effects of bedrock elevation and presence of coastlines.

The time scale for adjustment is $1/2\omega$. In the steady state $h = \frac{1}{2}H^*$, which corresponds to an isostatic balance if the rock density is three times that of ice [this ratio was for example used by Weertman (1976), who included instantaneous isostatic adjustment in a perfectly plastic ice sheet model].

Equation (15) is a very crude representation of what happens in the earth's upper mantle, because the adjustment is assumed to be local. A more sophisticated treatment of bedrock sinking has recently been described by Ghil and Le Treut (1980), but it has not yet been implemented in the present ice sheet model.

For the experiment to be discussed now, eq. (15) serves the purpose: the bedrock sinks or rises to restore the isostatic balance, and this mechanism has an $e$-folding time scale of $\tau = 1/2\omega$.

Consider the situation of Fig. 5 again. To mimic a situation of temporary low insolation in the Northern Hemisphere high latitudes, in the model $P$ is moved southward, is kept on the continent for some time and is then moved northward again into the polar sea. The upper curve of Fig. 12 shows this prescribed movement of the climate point. The subsequent curves show how the ice sheet reacts to this forcing for different values of $\tau$. Values of the model parameters are: $m = 2.5$, $A = 3\ \mathrm{m^{-3/2}\ yr^{-1}}$, $\theta = 0.5*10^{-3}$; initially $h(x) = 0$.

In the case of no bedrock adjustment ($\tau = \infty$) the ice sheet grows to a steady state in about 40,000 years. Apparently, if the climate point shifts into the polar sea again, the height of the ice sheet is already sufficient to keep the mass balance of the sheet positive. If isostatic adjustment with a long time scale is included ($\tau = 30{,}000$ years), the picture changes drastically. The ice sheet grows during about 50,000 years, but then the bedrock has sunk so much that a large part of the ice surface comes below the equilibrium line which causes the ice sheet to decay rapidly. For smaller time scales for bedrock sinking, this feature occurs earlier.

The "spontaneous" decay of a large ice sheet due to bedrock sinking is of great importance in explaining the Pleistocene glacial cycles. It can provide an explanation for the sawtooth shape of the dominant 100,000 years cycle in the oxygen isotope record (Hays et al., 1976). For a further discussion on this point, see Oerlemans (1980b).

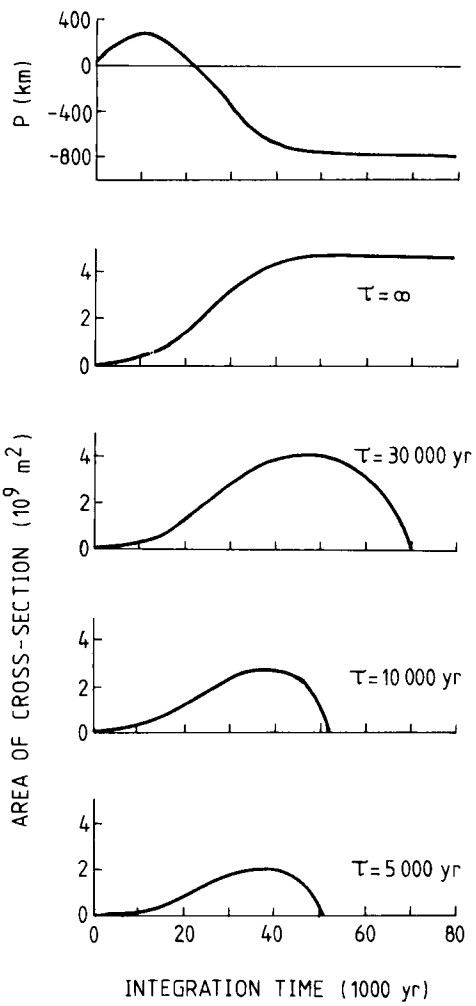


*Fig. 12.* Model experiments on the effect of bedrock sinking. The upper curve shows the prescribed movement of the climate point $P$ (compare Fig. 5). The other curves shows the corresponding evolution of a Northern Hemisphere ice sheet, for different values of the e-folding time scale for isostatic adjustment ($\tau$).

## 8. Discussion

The experiments discussed in this paper have shown that an ice sheet with very simple dynamics can react strongly nonlinear to changing climatic conditions. Although the model for ice flow used does not contain many internal degrees of freedom, the boundary conditions and the height of dependence $G$ create a rather complicated behaviour of the (model) ice sheet. This behaviour may be drastically changed again if bedrock sinking is included.

As stated earlier, the goal of this article is to show some basic characteristics of large ice sheets which are relevant from the viewpoint of dynamic climatology. The material presented here is somewhat theoretical, real case studies have not been carried out. However, the results give insight into the effects of geometry and orography, and this can be applied to real situations. A few inferences are made below.

The Antarctic and Greenland Ice Sheets have one point in common: they are both bounded by ocean. According to the model results displayed in Fig. 3, those sheets will be comparatively insensitive to variations in the mass balance. This applies up to a certain critical point, however. If during some extremely intense climatic warming the height of the equilibrium line increases so much that the total mass balance of the sheet becomes negative, the ice sheet will of course disappear. If this would happen for example with the Greenland Ice Sheet, it would probably not be built up again if conditions would return to to those of the present climate. It is obvious that a solution diagram for ocean-bounded ice sheets must also show hysteresis.

The Northern Hemisphere continental ice sheets that are present during glacials (the Laurentide and Eurasian Ice Sheets) are of a very different nature. Since those sheets are not bounded by ocean in the south, the slope of the equilibrium line becomes dominating. In contrast to the Antarctic and Greenland Ice Sheets, the Laurentide and Eurasian sheets are much more sensitive to variations in climatic conditions. Geological evidence for this is abundant (e.g. Flint, 1971).

Finally, the results of this study point to the extreme importance of bedrock sinking in the evolution of the Northern Hemisphere ice sheets. As was already mentioned by Weertman (1961), this may be the clue in explaining the quaternary glacial cycles as they appear in the oxygen isotope record.

## 9. Acknowledgements

I thank Cor Schuurmans, Theo Opsteegh and the reviewers for their valuable comments on an earlier version of this paper.

## REFERENCES


Andrews, J. T. and Mahaffy, M. A. W. 1976. Growth rate of the Laurentide ice sheet and sea level lowering (with emphasis on the 115,000 BP sea level low). *Quaternary Research 6*, 167–183.

Birchfield, G. E. 1977. A study of the stability of a model continental ice sheet subject to periodic variations in heat input. *J. Geophys. Res. 82*, 4909–4913.

Bodvarsson, G. 1955. On the flow of ice sheets and glaciers. *Jökull 5*, 1–8.

Budd, W. F. and Radok, U. 1971. Glaciers and other large ice masses. *Rep. Progr. Phys. 34*, 1–70.

Charlesworth, J. K. 1957. *The quarternary era*. Edward Arnold Ltd., London.

Flint, R. F. 1971. *Glacial and quaternary geology*. Wiley, New York.

Ghil, M. and Le Treut, H. 1980. *A climate model with cryodynamics and geodynamics*. Laboratoire de Météorologie Dynamique (CNRS), LMD Note 104.

Hays, J. D., Imbrie, J. and Shackleton, N. J. 1976. Variations in the earth's orbit: pacemaker of the ice ages. *Science 194*, 1121–1132.

Imbrie, J., Van Donk, J. and Kipp, N. G. 1974. Comparison of isotope and faunal methods: palaeoclimatic investigation of a late pleistocene Carribean deep-sea core. In: *Mapping the atmospheric and oceanic circulations and other climatic parameters at the time of the last glacial maximum about 17,000 years ago*. Climate Research Unit, Norwich, 6–9.

Nye, J. F. 1959. The motion of ice sheets and glaciers. *J. Glaciol. 3*, 493–507.

Oerlemans, J. 1980a. Modelling of Pleistocene European ice sheets: some experiments with simple mass balance parameterizations. *Quaternary Research*, in press.

Oerlemans, J. 1980b. Model experiments on the 100,000 yr glacial cycle. Submitted to *Nature*.

Oerlemans, J. and Bienfait, J. M. 1980. Linking ice-sheet melting to Milankovitch radiation variations: a simple model study. To appear in proceedings of the "*Sun and Climate*" conference, Toulouse, fall 1980.

Paterson, W. S. B. 1969. *The physics of glaciers*. Pergamon, Oxford.

Pollard, D. 1978. An investigation of the astronomical theory of the ice ages using a simple climate-ice sheet model. *Nature 272*, 233–235.

Weertman, J. 1961. Stability of ice-age ice sheets. *J. Geophys. Res. 78*, 4463–4471.

Weertman, J. 1976. Milankovitch solar radiation variations and ice age ice sheet sizes. *Nature 261*, 17–20.


## НЕКОТОРЫЕ ЭКСПЕРИМЕНТЫ С ВЕРТИКАЛЬНО ПРОИНТЕГРИРОВАННОЙ МОДЕЛЬЮ ЛЕДНИКОВОГО ЩИТА


Предлагается простая $1\frac{1}{2}$ мерная модель континентального ледникового щита. Модель основывается на предложении Ная (1959) выражать осредненную по вертикали горизонтальную скорость льда как $u = B\tau_b^m$, где $\tau_b$—касательное напряжение у основания ледника, а $B$ и $m$—постоянные. Существенно, что распространение льда управляется нелинейным уравнением диффузии для толщины льда. Диффузионная способность возрастает как с ростом толщины льда, так и наклона его поверхности. В одном направлении ($y$) предписывается типичный масштаб, который регулирует горизонтальный сток массы льда, тогда как в другом направлении ($x$) эволюция ледникового щита подробно вычисляется на сетке с шагом в 70 км.

Был выполнен ряд экспериментов с различными граничными условиями и параметризациями годового баланса массы. Оказывается, что ограниченность континентов и профили подстилающей поверхности создают сильно нелинейную реакцию ледниковых щитов на климатические изменения. Поведение ледниковых щитов в Северном полушарии, рассчитанное с помощью численной модели, сравнивается с поведением, предсказываемым моделью идеальной пластичности. Найдено, что эти модели дают качественно одинаковые результаты.